Application of Magnetic Resonance Fingerprinting to Measure Brain Oedema

Jack Allen
Supervisors: James Kennedy & Peter Jezzard

Oxford-Nottingham Biomedical Imaging Centre for Doctoral Training
University of Oxford
United Kingdom
2nd October 2015

Application of Magnetic Resonance Fingerprinting to Measure Brain Oedema

Student: Jack Allen* *Supervisors:* James Kennedy† & Peter Jezzard*

***Abstract*—**

***Index Terms*—Magnetic Resonance Imaging Fingerprinting, Stroke**

I. Introduction

Magnetic resonance imaging (MRI) has become an established and widely used tool for producing images for diagnosis and disease monitoring in clinical environments. Differences between tissue types are often highlighted qualitatively via image contrast, but efforts are being made to produce more quantitative parameter measurements. Two commonly extracted properties are the terms that describe the rate at which the transverse and longitudinal magnetisation components evolve over time (T_2 and T_1, respectively). The time constant T_2 can be measured by conducting a spin echo (SE) experiment and varying the echo time TE at which the signal is recorded. Equation 1 describes how the evolution of the transverse magnetisation M_{xy} depends on TE and T_2. The value of T_2 can be extracted from a fit of eq. 1 to the detected signal evolution.

[1].

$$M_{xy}(TE) = M_{xy}(0)\exp^{-\frac{TE}{T_2}} \tag{1}$$

Inversion recovery (IR) sequences are often used to measure T_1. During an IR experiment, the fully relaxed equilibrium longitudinal magnetisation M_0 is rotated by 180^o, so that its sign becomes negative. Equation (2) describes the evolution of M_z over the time t after the inversion. Given sufficient time, M_z will return to M_0. By varying the inversion time TI at which the signal is detected, the evolution of M_z over time can be obtained and T_1 can be determined by fitting (2) to the measured data point.

$$M_z(t) = M_0(1 - 2e^{-\frac{t}{T_1}}) \tag{2}$$

Implementations of traditional T_1 and T_2 measurement methods also must deal with factors that can potentially cause measurement errors, such as subject movement and field inhomogeneities. Also, these methods usually require large scan durations, although in recent years simultaneous multi-parameter measurements have been made in only 5 minutes [2].

Recently, a new approach known as magnetic resonance fingerprinting (MRF) has been developed and applied, which has been used to simultanously measure multiple parameters, such as T_1 and T_2, with a reduction in the scan time needed. The method seems to cope very well with subject movement and it is also claimed that the technique delivers an improvement in efficiency, compared to the previous best approaches [3], [4]. During a MRF experiment, a pseudo-random sequence is used to manipulate the spins in a sample and acquire images. This can be achieved by varying factors in the sequence, such the time in between subsequent RF pulses and the size of any rotations in the net magnetisation that may be induced by the RF pulses. Once a series of images have been acquired via a MRF sequence, the signal pattern for each pixel over the whole experiment is compared to a previously built dictionary of simulated signals patterns, in order to find the closest match. The dictionary is built by simulating the signal expected from the particular experiment type, for all combinations of the chosen parameters (such as T_1 and T_2), over given ranges for each parameter.

MRF has been used to provide quantitative measurements in a variety of different imaging scenarios, for a range of different organs. Many of the applications have been in areas of clinical imaging, where the improved speed and repeatability is especially appealing. However, there is scope for MRF to be used within the setting of emergency medicine, where fast diagnosis and treatment is even more important for improving the prognosis of a patient. The knowledge gained from imaging in this environment is crucial for ensuring accurate diagnosis and informing decisions for subsequent treatment. Qualitative images are widely used, but quantitative measurements would provide more information on physiological changes and would increase the robustness of the classification of tissue. For example, the measured properties of the tissue within each voxel could be compared to an expected range of values for particular pathologies. The consistency of tissue classification across different scans, as well as between medical centres, could be improved. Specifically, acute stroke patients could benefit from the advantages of MRF. Stroke is a major cause of death, but can also have large negative effects on the quality of life of those who survive. The localised reduction in blood supply that occurs during a stroke can cause a region of cells to become damaged or die, but if the patient is treated quickly, the surrounding areas may be salvageable. Treatment is usually given by administering drugs that are designed to break down clots that may be blocking the blood vessels and there is a window of approximately 3 hours within which this treatment will improve the outcome of the patient [5]. MRF can be used to locate the damaged area via the simultaneous measurement of multiple parameters, with the choice of parameters ensuring

*FMRIB Centre, Nuffield Department of Clinical Neurosciences, University of Oxford, Oxford, UK.
†Radcliffe Department of Medicine, University of Oxford, Oxford, UK.

	Homogeneous Phantom Sample Pixels					
	1	2	3	4	5	6
T1 [ms]	282	282	283	283	282	282
T2 [ms]	216	215	214	215	214	215

TABLE I: Measured properties for the sample pixels in the homogeneous phantom.

	Custom Phantom Compartments					
	1	2	3	4	5	6
Deionised Water [ml]	50	50	50	50	50	50
Agar [g]	1.05	0.76	0.00	2.00	1.64	1.31
Nickel Chloride [g]	0.19	0.13	0.00	0.65	0.39	0.26
T1 [ms]	190	253	3127	60	118	126
T2 [ms]	73	98	2039	19	41	54

TABLE II: Concentrations and measured properties for the compartments in the custom phantom.

a range of different perspectives on tissue health. For example, the build up of extracellular water (i.e. Oedema) is an indicator of cell damage [6], [7]. Quantities of water can be inferred from M_0 measurements and then co-registered with maps of other properties, such as T_1 and T_2.

In this work, we used the MRF approach to make measurements of T_1, T_2, M_0 and B_1 deviation, for phantoms with a range of T_1 and T_2 values. We assessed the performance of our algorithm for various sequences and considered its potential to be used to produce quantitative images for the assessment of acute stroke.

II. Materials and Method

A. Phantom production

We made a phantom, with the aim of that it would mimic some the variation that is present in brain tissue. Our custom phantom contained six different compartments, each designed to have different T_1 and T_2 values. This variation allowed us to explore the ability of MRF to measure a range of properties within one sample. Nickel Chloride and Agar were used to produce a range of T_1 and T_2 values, as reported in [8]. The phantom comprised six conical tubes within a 4L high-density polyethylene (HPDE) container. The conical tubes were secured in the centre of the larger vessel by a plastic 3D printed structure. The liquid that surrounded the small compartments was between 0.9% and 1.0% m/v Sodium Chloride in Deionised water. This concentration was chosen to mimic the levels that are generally found in the human body (i.e. physiological saline). Each of the smaller compartments contained different concentrations of the same ingredients, as described in Table II. Figure 1 demonstrates the numbering of the compartments.

B. Image acquisition

Images were acquired of two phantoms: a homogeneous spherical phantom and our custom phantom. The spherical phantom contained Nickel(II) Sulfate Hexahydrate in distilled water, at a concentration of 0.125% m/m. The uniformity of the spherical phantom meant that is was useful for initial tests

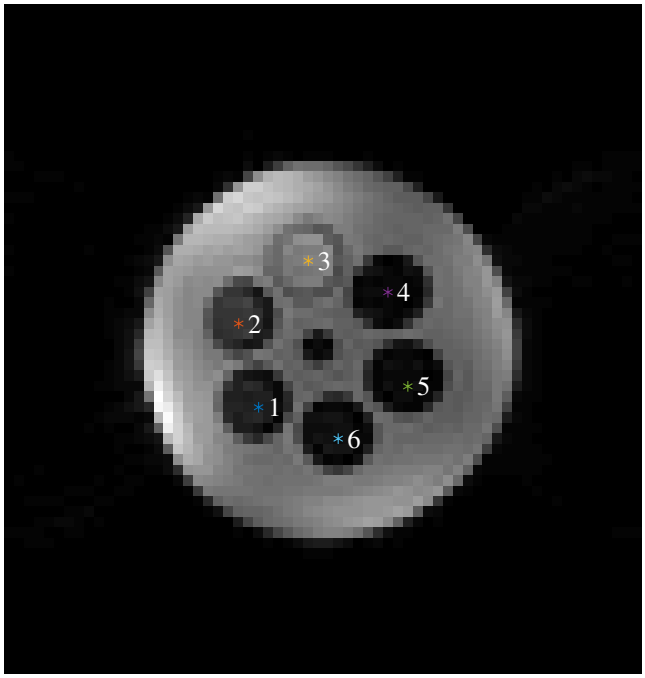

Fig. 1: An example image from the T_1 measurements of the custom phantom. The compartments are numbered and the sample pixels are marked as stars. The numbering of the compartments was the same for the T_1 and T_2.

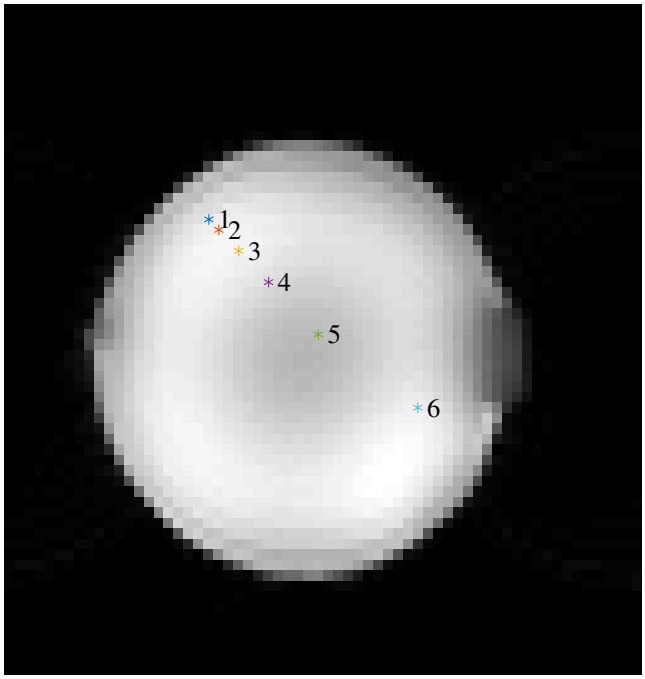

Fig. 2: The positioning of the sample pixels for the T_1 and T_2 measurements of the homogeneous phantom. The six sample pixels are marked as stars.

of the algorithm, because if the method is working there should be minimal variation in the assigned T_1 and T_2 across the phantom.

All images were acquired at the Acute Vascular Imaging Centre (AVIC) at the John Radcliffe Hospital in Oxford, using a 3T Siemens Verio magnet and a 12 channel Siemens head coil. Conventional inversion recovery (IR) and spin echo (SE) experiments were performed, using various values of TI and TE, respectively. The images that were acquire from these experiments were later used to extract "gold standard" T1 and T2 values.

To produce the MRF images, a list of timings was used to control a SE experiment. The list was pseudo-random and controlled the TE and TR, as well as the first and second flip angles (FA_1 and FA_2), for the acquistion of each image.

The fingerprinting sequence excited two slices of the sample. It also involved a fat saturation pulse before the first proton pulse, as well as crusher gradients at the end of each repetition, designed to remove any residual transverse magnetisation. The experiment involved the aqcuisition of 48 images, via 48 repetitions.

TABLE III: Sequence Control List

Image Index	TE [ms]	TR [ms]	FA1 [degrees]	FA2 [degrees]
1	10000	0	90	180
2	220	240	90	180
3	20	800	90	160
4	60	620	90	180
5	360	160	50	180
6	80	560	90	180
7	100	500	90	180
8	120	440	30	40
9	160	360	90	180
10	180	320	90	180
11	700	40	90	180
12	200	280	90	180
13	140	400	60	130
14	240	220	90	180
15	280	200	90	180
16	320	180	90	150
17	400	140	90	180
18	440	120	20	180
19	500	100	90	180
20	560	80	90	180
21	40	700	90	160
22	620	60	70	180
23	800	20	90	180
24	800	0	90	180

C. T_1 and T_2 extraction

Firstly, the IR and SE images of the two phantoms were used to measure T_1 and T_2, respectively. The curves in eq. (2) and eq. (1) were fitted to the signal timecourse of particular pixels in their corresponding sets of images, using MATLAB (The MathWorks, Natick, MA). For the homogeneous phantom, these sample pixels were spread across the phantom, as shown in Fig. 2. For the custom phantom, the pixels were at fixed coordinates within each of the six compartments. As an example, the sample pixels for the measurement of the T_1 of the custom phantom are marked in Fig. 1.

D. Dictionary creation

Using MATLAB, dictionary entries were simulated with the timings list.The simulation code was based on a mathematical description of a refocusing pulse, found in [9]. This description was adapted so that it could be used to simulate the signal from a SE experiment within more than one TR. To test that the simulation was working correctly, comparisons were made between the first 24 simulated and observed signal values. This was done by using the gold standard T_1 and T_2 values to calculate the expected values for each image of the homogeneous phantom and plotting them with the signals from the sample pixels.

The values of T_1 and T_2 used to create the dictionary for the homogeneous phantom were between 200ms and 300ms, in increments of 10ms. The ranges of these parameter values was designed to include values below and above the gold standard measurements. In order to account for variations in the B_1 excitation field, a range of deviations from each intended flip angle was also used to produce the dictionary entries. This range was $\pm 30\%$, in increments of 1%. It was assumed that these deviations at a particular pixel would be constant for each pulse through out the sequence. As a result of producing signals with each possible combination of these three parameters, each dictionary for the homogeneous phantom contained 7381 entries. The dictionary for the custom used the same increments and B_1 values, but the T_1 and T_2 ranges needed to be extended. The ranges of T_1 and T_2 were both 10ms to 120ms and 1900ms to 2100ms. The dictionary for the custom phantom comprised 19764 signal patterns. The dictionaries for the homogeneous and the custom phantoms took 8 and 21 minutes to compile, respectively. The computations were performed using a commercial portable computer, with a 2.6Hz processor and 4 cores.

E. Signal matching

For a given pixel within the field of view, we compared each dictionary entry $\vec{D}$ with the first 24 points of the signal timecourse $\vec{S}$ at that pixel, to see which dictionary pattern was the most similar. As is reported in the original MRF publication [3], we used the dot product of each pair of compared vectors, with an aspect of normalisation, to calculate similarity scores. The specific expression that we used for our similarity calculations is shown in eq. 3, where the resulting similarity score $\cos(\theta)$ is restricted to values between 0 and 1. An exact match would give a score of 1. By dividing the product of the vector norms, the bias towards vectors with large data values was reduced. The intention for reducing this bias was that high similarity scores would highlight the dictionary entry and timecourse pair with the most similar type of pattern variations. Once the entry that gave the highest similarity score was found, the corresponding parameters T_1, T_2 and B_1 were assigned to that particular pixel. Good performance was defined as a close match between the assigned T_1 and T_2 and the gold standard values. An indication of the proton density M_0 was calculated as the mean of the scaling factors for the pairs of corresponding points in the best matched entry and the signal timecourse. The absolute scaling factor values

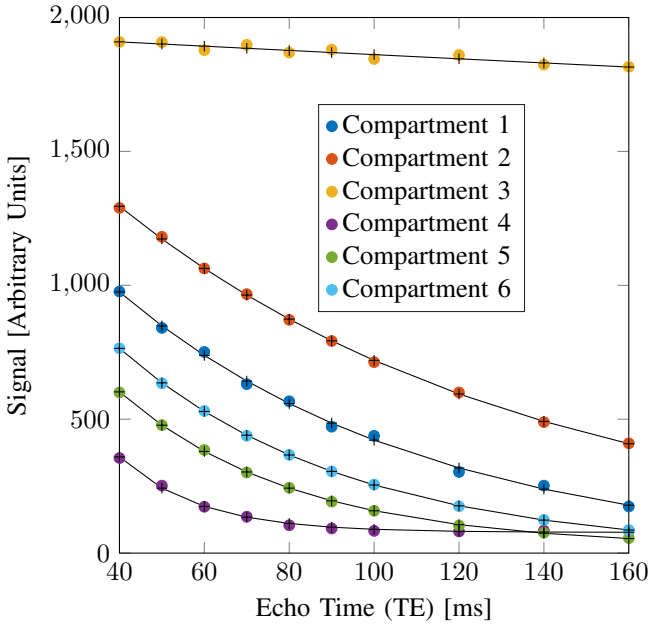

Fig. 3: T2 decay curve fitted to the measurement data for each compartment in the phantom. The fitted points are represented by plus symbols.

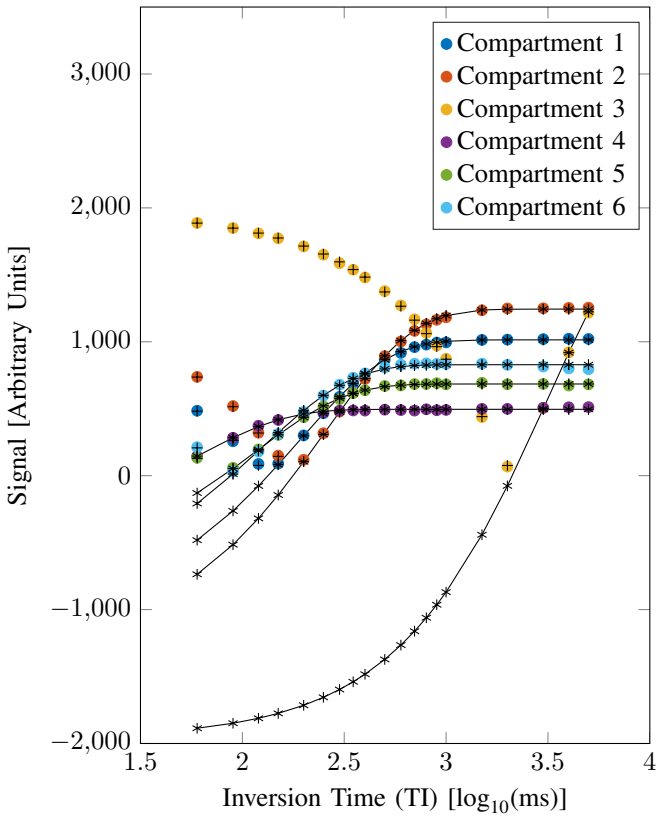

Fig. 4: Sign sensitive T1 recovery curves, for each compartment in the phantom. A log scale for the x-axis is used for clarity. The magnetisation fits are plotted (stars), along with its absolute values (plus marks).

were used for this calculated, as unfortunately some of the simulated signal points were negative. After a circular mask had been applied to the phantoms, the entire matching process was performed for all the pixels that had not been excluded. Our algorithm took approximately 3 and 5 minutes to find the best matches for 1257 pixels in the images of the homogeneous and custom phantoms, respectively.

$$\frac{\vec{S}\cdot\vec{D}}{\|\vec{S}\|\|\vec{D}\|} = \cos\theta \tag{3}$$

III. Results and Discussion

A. Gold standard T1 and T2

Figures 4 and 3 show the T_1 and T_2 fits for the custom phantom signals. The signal curves in Fig. 3 and Fig. 4 all have different initial values, suggesting that the inital longitudinal magnetisation was not at a fully relaxed equilibrium. Also, from Fig. 3 it is clear that the chosen echo times were not great enough to allow for a significant decay in the signal from the deionised water in compartment 3. These factors could have skewed the gold standard measurements, but the fitting curves seem to closely match the data.

B. Simulation Testing

Simulation matches slice 2 better than slice 1, in particular, Images 11 and 22 *Slice 2 data matches the simulation well* *greater variation in signal for images 5, 11, 13, 16, 18, 22. Could be caused by combination of small FA1 compared to FA1?*

C. Property Maps

The signal dictionary that was used to produce the parameter maps in Figs. 6a and 6b took approximately 5 minutes to create. The similarity calculations for the same list required approximately 10 minutes.

Ideally, the scaling factors would be identical for all the pairs of corresponding points within the best matched dictionary entry and the data for a given pixel. However, the scaling factors were different for each image. Because of this, the mean of the scaling factors was used to indicate M_0.

state how long the scan took

In the future we should remake the Phantom so that it has T1 and T2 that are found in the brain *comment on further work: improving accuracy of algorithm. apply in vivo, possibly try different sequence styles* Once our method has been refined, it is important that it used to apply MRF in vivo, to work towards the goal of implementing the approach at the AVIC. *things that the original paper did differently to me or I left out?* *issues that i had that others also had?* Previous MRF studies have used a much larger dictionary than we have used in this work. This could improve the ability of our implentation to successfully measure the properties of interest. The simulation could be rewritten so that it only computes the signal that is nessecary for the simulation. This would reduce the required computation time, which is a factor that

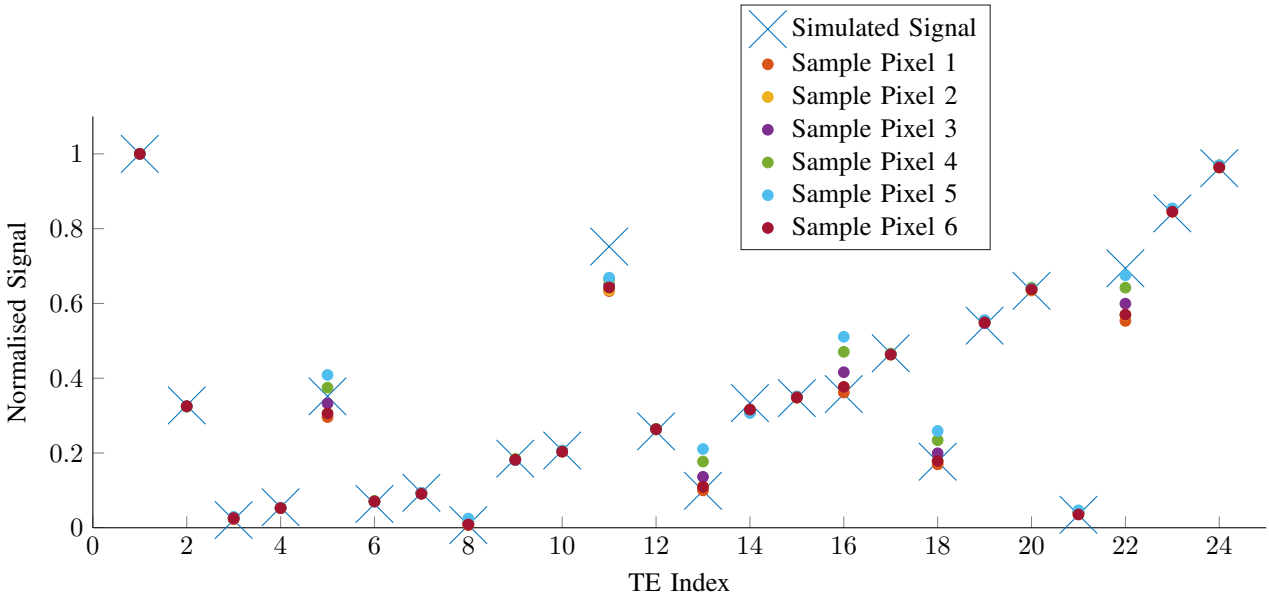

(a) Slice 1

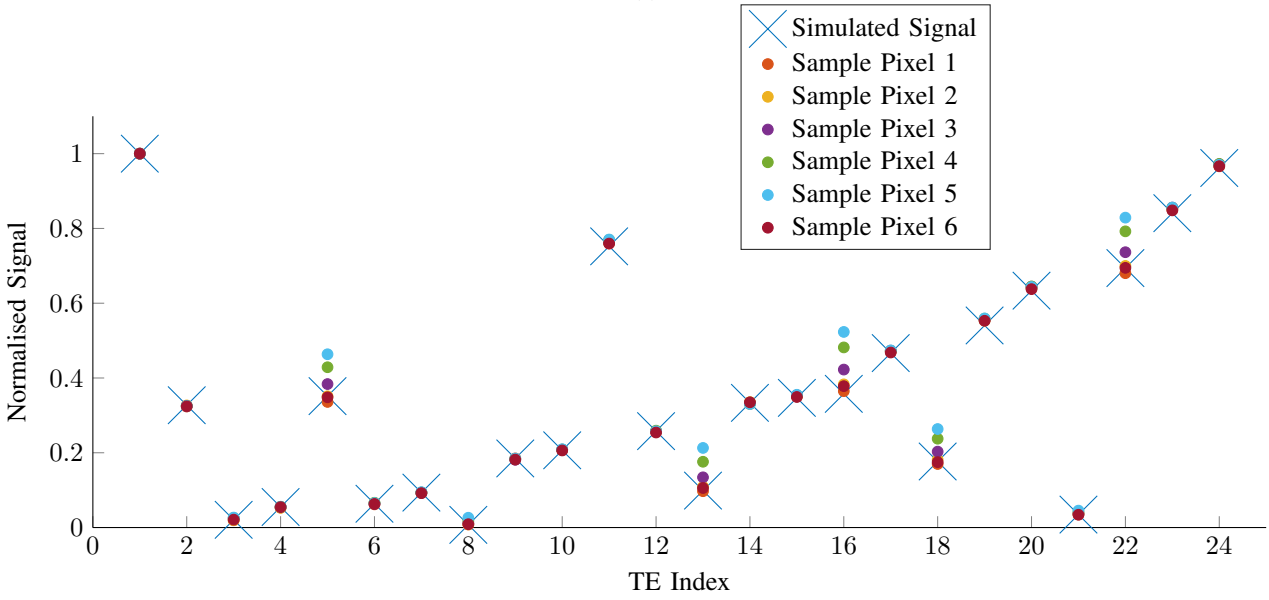

(b) Slice 2

Fig. 5: Comparison of the simulated and acquired signal, for the two slices of the homogeneous phantom, for each of the six sample coordinates

would become more significant if the size of the dictionary is increased.

T1 didn't match as well asT2...could be because the TR offset times in the timings list were long compared to the T1 values, so not much difference in Mz at each TE *M0 is not too bad, but need to resolved the problem of negative values...*

sped up by reducing the range of properties of interest *could speed up matching process by storing simulate signal vectors in a 2D matrix, and using parallel for loop, instead of two nested For loops...*

IV. Conclusions

Comment on the potential for this to be used in AVIC

V. Acknowledgements

Robert Brand for providing the design for the phantom. Sam Hurley for his T_1 fitting software.

References

[1] E. M. Haacke, R. Brown, M. Thompson, R. Venkatesan, Magnetic resonance imaging: physical principles and sequence design., New York: A John Wiley and Sons.

[2] J. Warntjes, O. D. Leinhard, J. West, P. Lundberg, Rapid magnetic resonance quantification on the brain: Optimization for clinical usage, Magnetic Resonance in Medicine 60 (2) (2008) 320–329. doi:10.1002/mrm.21635.
URL http://dx.doi.org/10.1002/mrm.21635

[3] D. Ma, V. Gulani, N. Seiberlich, K. Liu, J. L. Sunshine, J. L. Duerk, M. A. Griswold, Magnetic resonance fingerprinting, Nature 495 (7440) (2013) 187–192.

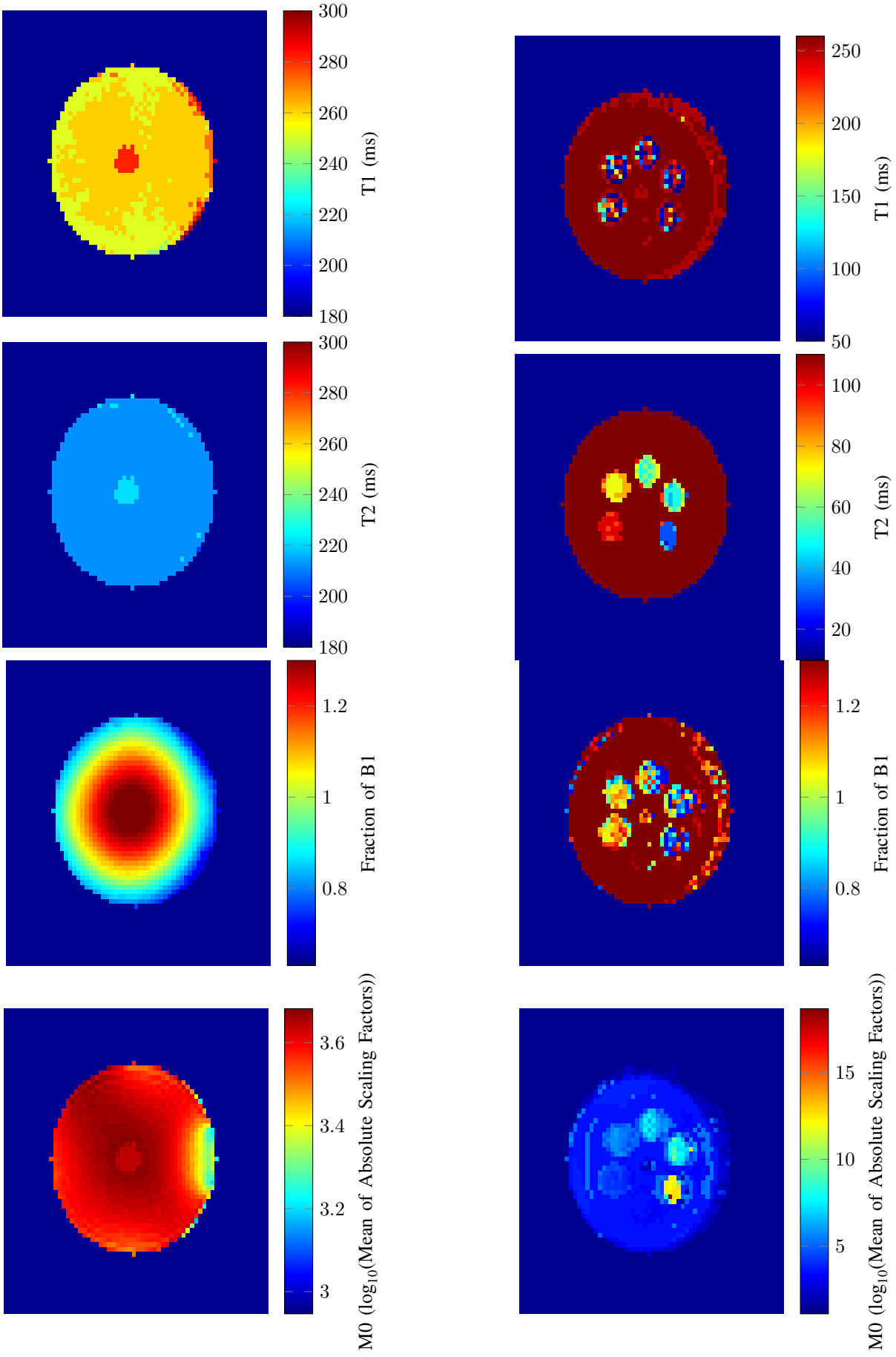

(a) Homogeneous phantom

(b) Custom phantom

Fig. 6: Parameter maps for slice 2 of each phantom.

[4] S. C. Deoni, T. M. Peters, B. K. Rutt, High-resolution t1 and t2 mapping of the brain in a clinically acceptable time with despot1 and despot2, Magnetic resonance in medicine 53 (1) (2005) 237–241.
[5] B. S. Alper, M. Malone-Moses, J. S. McLellan, K. Prasad, E. Manheimer, Thrombolysis in acute ischaemic stroke: time for a rethink?, BMJ 350 (2015) h1075.
[6] G. Harston, N. Rane, G. Shaya, S. Thandeswaran, M. Cellerini, F. Sheerin, J. Kennedy, Imaging biomarkers in acute ischemic stroke trials: a systematic review, American Journal of Neuroradiology 36 (5) (2015) 839–843.
[7] C. Ayata, A. H. Ropper, Ischaemic brain oedema, Journal of Clinical Neuroscience 9 (2) (2002) 113–124.
[8] L. Cochlin, A. Blamire, P. Styles, Dependence of t1 and t2 on high field strengths in doped agarose gels; facilitating selection of composition for specific t1/t2 at relevant field., in: Proc. Intl. Soc. Mag. Reson. Med, Vol. 263, 2003, p. 266.
[9] M. A. Bernstein, K. F. King, X. J. Zhou, Handbook of MRI pulse sequences, Elsevier, 2004.